EPORT DOCUMENTATION PAGE

AD-A217 597

E

1b. RESTRICTIVE MARKINGS

3. DISTRIBUTION/AVAILABILITY OF REPORT

4. PERFORMING ORGANIZATION REPORT NUMBER(S)

5. MONITORING ORGANIZATION REPORT NUMBER(S)

AFOSR-TR- 89-1857

6a. NAME OF PERFORMING ORGANIZATION	6b. OFFICE SYMBOL (If applicable)	7a. NAME OF MONITORING ORGANIZATION
Wayne State University		Air Force Office of Scientific Research

6c. ADDRESS (City, State and ZIP Code)	7b. ADDRESS (City, State and ZIP Code)
Detroit, MI 48202	Bolling AFB DC 20332-6448

8a. NAME OF FUNDING/SPONSORING ORGANIZATION	8b. OFFICE SYMBOL (If applicable)	9. PROCUREMENT INSTRUMENT IDENTIFICATION NUMBER
AFOSR	NA	AFOSR 83-0164

8c. ADDRESS (City, State and ZIP Code)

BOLLING AFB DC 20332-6448

10. SOURCE OF FUNDING NOS.

PROGRAM ELEMENT NO.	PROJECT NO.	TASK NO.	WORK UNIT NO.
61102F	2308	D9	

11. TITLE (Include Security Classification) AFTERBURNING SUPPRESSION KINETICS IN ROCKET EXHAUST

12. PERSONAL AUTHOR(S)
SINGH

13a. TYPE OF REPORT	13b. TIME COVERED	14. DATE OF REPORT (Yr., Mo., Day)	15. PAGE COUNT
FINAL	FROM 01JAN83 TO 30JUN83	UNDTD	

16. SUPPLEMENTARY NOTATION

17	COSATI CODES		18. SUBJECT TERMS (Continue on reverse if necessary and identify by block number)
FIELD	GROUP	SUB. GR.	

19. ABSTRACT (Continue on reverse if necessary and identify by block number)

DTIC
ELECTE
JAN 0 4 1990
S B D

90 01 04 188

20. DISTRIBUTION/AVAILABILITY OF ABSTRACT	21. ABSTRACT SECURITY CLASSIFICATION
CLASSIFIED/UNLIMITED ☐ SAME AS RPT. ☐ DTIC USERS ☐	

22a. NAME OF RESPONSIBLE INDIVIDUAL	22b. TELEPHONE NUMBER (Include Area Code)	22c. OFFICE SYMBOL
LEONARD H CAVENY	(202) 767-4937	AFOSR/NA

DD FORM 1473, 83 APR EDITION OF 1 JAN 73 IS OBSOLETE.

Afterburning Supression Kinetics in Rocket Exhaust

Sponsored by the

AIR FORCE OFFICE OF SCIENTIFIC RESEARCH

Prepared by: Trilochan Singh

Academic Rank: Associate Professor

Department: Mechanical Engineering Department

University: Wayne State University
                    Detroit, MI   48202

USAF Research
Colleague: Dr. Jay Eversole

AFTERBURNING SUPRESSION KINETICS IN ROCKET EXHAUST

1. INTRODUCTION

The exhaust gases from the nozzel of a rocket motor usually contain significant proportions of unburned fuel. This fuel mixes turbulently with ambient air as the exhaust jet expands and may burn causing a substantial elevation of temperature in the exhaust plume. The secondary combustion is affected by factors such as velocity and altitude of the missle, motor thrust level, pressure, temperature at the nozzle exit plane. The addition of certain species such as HBR, K_2SO_4 etc. have been observed to inhibit the afterburning process. The inhibition of afterburning process is ot great significance to the US Air Force. However, the kinetic mechanism for the afterburning suppression is not understood. A research program has been initiated at the Rocket Propulsion Laboratory to investigate the afterburning suppression kinetics by Dr. Jay Eversole. The fundamental research objective will be to determine the chemical reaction mechanisms that are critical to this afterburing suppression phenomena.

2. APPROACH AND OBJECTIVE

The experimental approach is to use a premixed flat flame burner and monitor the temperature profile, species profile (as a function of distance above the burner surface), burner surface temperature, and flow velocity. The construction of the apparatus is nearly complete and data acquisition for atmospheric flames is expected in the near future at the Rocket Propulsion Laboratory.

It is essential that the experimental approach be supported by a computational model. The objective of the principal investigator's summer assignment in 1982 at the AFRPL was to study the feasibility of the experiment by using an appropriate set of computer programs. A review of the literature showed that a computer code PLFLAME with some modifications would be suitable for the proposed experiment under construction.

PLFLAME code was obtained through Dr. Terence P. Coffee of the US Army Ballistic Research Laboratory, Aberdeen Proving Ground, Maryland in mid-June 1982. PLFLAME code simulates the combustion process occuring in the laminar, premixed, one dimensional steady state flame. PLFAME code is divided into four sequential parts.

The first part requires thermochemical data (such as given in JANAF

1

thermochemical tables) and the transport properties data (such as Lennard-Jones potential parameters) for all the reaction species in the reaction scheme as input. This first part of the PLFLAME code produces a data file containing a set of coefficients for the various polynomial fits used for calculating the transport properties of the species as a function of temperature. This data file is used as input to the second part of the PLFLAME code. The mole fraction for the incoming stream, the inlet temperature and the pressure are given as input by the user. PLFLAME code part I also generates three subroutines RT, RATE and F which are used by part II and part III. These subroutines calculate the rates of forward reactions and the backward reactions involved in the proposed mechanism.

PLFLAME code II generates a set of data containing the inlet boundry conditions (unburned gas compostion, unburned gas temperature, pressure and flow velocity), burned gas adiabatic flame temperature and the corresponding equilibrium composition. The latter data serves as boundry condition at the hot end of the flame.

The output of the PLFLAME II is used as input to the PLFLAME III. The user also supplies the numerical parameters such as the number of breakpoints, number of continuity equations of each collocation point, spatial and temporal error tolerance, final nondimensional distance from the flame center or the burner surface and the ratio between the longest interval and the shortest interval for the break points. PLFLAME III numerically solves a set of coupled differential equations governing a laminar, premixed, one dimensional, steady state flame. The basic procedure is to integrate the equations in time till a steady state solution is obtained. Coffee (2) describes in detail the partial differential equations governing the flames and the meth of solution used in the code. PLFLAME IV produces graphs of the temper   e distribution and the mole fraction distribution of the various species as a function of the distance. During the summer of 1982 the principal investigator was able to bring the PLFLAME code in satisfactory working mode on the AFRPL computing system.

The goal of this project (AFCSR-83-0164 Contract) was to validate the PLFLAME code by comparing the calculated results with the experimental results reported in the literature. The calibrated program was then used for investigating the suppression kinetic meachanism for candidate species like K, HBR, KOH. The sensitivity of the results were investigated by

2

varying the reaction rate data and the transport data.

3.0 PLFLAME CODE VALIDATION FOR H2/02/N2 SYSTEM

At present, the hydrogen-oxygen flame is the only flame for which
the rate constants of the elementary reactions are known with reasonable
accuracy. A review of the literature shows that only a limited amount
of experimental data are available for H2-02-N2 flames. Dixon-Lewis (3)
has given a detailed review of the kinetic mechanisms, structure and
properties of the premixed flames in H2-02-N2 system. The output of
the PLFLAME gives the adiabatic flame temperature and the corresponding
equilibrium composition of the burned gas, temperature profiles, species
profiles and the flame velocities. The computed results of the PLFLAME
code are compared with those reported in the literature. The validation
procedure evolved into four parts: a) adiabatic flame temperature to
other calculational results, b) sensitivity of PLFLAME results to numeri-
cal parameters, c) comparison of the PLFLAME flame speed both to other
computations and to experimental results d) comparison of the PLFLAME
equilibrium composition.

3.1 EQUILIBRIUM COMPOSITION AND ADIABATIC FLAME TEMPERATURE

PLFLAME II calculates the adiabatic flame temperature and the corres-
ponding equilibrium composition. Table 1 shows the comparison between
PLFLAME II results and those reported by Jensen and Jones (4)

TABLE 1

Unburned Mole Ratio H2/N2/02/K	$H2O \times 10^{-17}$ Molecules		$H2 \times 10^{-17}$ / CM^3		$H \times 10^{-15}$		Eq. T °K	
	PL	Jen.	PL	JEN.	PL	Jen.	PL	Jen.
3.5/6./1./0.	8.6	8.6	6.3	6.4	0.5	0.7	1790	182
4.0/5./1./0.	8.8	8.6	8.6	8.6	1.1	1.7	1865	192(
5.0/3./1./0.	9.0	8.9	13.4	14.0	4.4	5.2	2032	205!
4.5/3.5/1./0.	9.1	8.9	11.2	11.0	4.0	4.6	2028	205!
4.0/4.0/1./0.	9.1	8.9	8.9	9.0	3.4	4.2	2024	205!
3.27/4./1./0.	9.4	9.3	5.9	6.1	5.8	6.8	2146	217(

PL = PLFLAME Code results

Jen = Jensen's Results (4)

3

The results obtained by using NASA equilibrium code (at Wayne State University and at AFRPL) are similar to those of PLFLAME Code. Table 1 shows good agreement between the PLFLAME Code results and those of Jensen (4).

3.2 EFFECT OF SOME NUMERICAL PARAMETERS INPUT TO PLFLAME III

PLFLAMF III uses the package PDECOL (2) to solve a general system of N nonlinear partial differential equations of at most second order on a finite interval. The spatial discretization is accompanied by finite element collocation methods based on B-Splines (2). The user has to supply the values of NINT, which determines the number of breakpoints, KORD, the order of splines, NCC, the number of continuity conditions to be applied at each point, and FC, the ratio between the longest interval and the shortest interval. For the cases studied in this report, we used NINT= 12 to 24, KORD=4, NCC=2 and FC= 4 to 6.

The calculations for the flame structure can be carried out to different distances from the center of the flame or from the burner surface by varying the value of non-dimensonal parameter PHR. For short distance (above the burner surface or from the centre of flame with PHR=0.5 to 1) NINT=12 was used. As PHR was increased to 3, NINT was increased to 20 to 24. Table 2A shows that the computed burning velocity for unbounded flames do not change as the calculations are carried with different limits of nondimensional distance parameter PHR. Table 2B shows the reaction rates and the reaction mechanism used for these calculations.

TABLE 2A

Effect of Nondimensional Distance PHR on Flame Velocity

Mole Ratio $H2/O2/N2$	PHR	X-mm	Flame Vel. Cm./Sec.
0.3/.15/.55	0.5	0.97	220.86
0.3/.15/.55	2.0	4.20	220.24
0.3/.15/.55	3.0	6.40	221.69

To obtain an accurate solution both the temporal accuracy and the spatial accuracy must be sufficient. Spatial accuracy is more important near the flame fronts where we have steep gradients. As the number of breakpoint (NINT) increases, the spatial errors decrease and the computation

4

Table 2B

Reaction Mechanism and Reaction Rates for

H2-O2-N2 System

$$R = A\, T^n \exp(E/T)\ cm^3\text{-moles-sec units}$$

		A	n	E
1	OH + H2 = H2O + H	1.1700E+09	1.3000E+00	-1.8250E+03
		1.2104E+10	1.1989E+00	-9.6237E+03
2	H + O2 = OH + O	1.4200E+14	0.	-8.2500E+03
		4.2321E+11	3.8707E-01	-4.6898E+02
3	O + H2 = OH + H	1.8000E+10	1.0000E+00	-4.4800E+03
		1.0182E+10	9.7038E-01	-3.4743E+03
4	H + O2 + MP = HO2 + MP	1.0300E+18	-7.2000E-01	0.
		2.0658E+18	-7.6048E-01	-2.3580E+04
5	H + HO2 = OH + OH	1.4300E+14	0.	-5.4000E+02
		5.1207E+10	6.6351E-01	-1.9370E+04
6	H + HO2 = O + H2O	1.0000E+13	0.	-5.4000E+02
		6.5269E+10	5.9504E-01	-2.8169E+04
7	H + HO2 = H2 + O2	1.2500E+13	0.	0.
		2.7012E+12	3.0654E-01	-2.8553E+04
8	OH + HO2 = H2O + O2	7.5000E+12	0.	0.
		1.6512E+13	2.0733E-01	-3.6349E+04
9	O + HO2 = OH + O2	1.4000E+13	0.	-5.4000E+02
		1.7090E+12	2.7708E-01	-2.8088E+04
10	O + HO2 = OH + O2	1.2500E+12	0.	0.
		1.5259E+11	2.7708E-01	-2.7548E+04
11	H + H + H2 = H2 + H2	9.2000E+16	-6.0000E-01	0.
		3.9061E+16	-3.3146E-01	-5.2130E+04
12	H + H + N2 = H2 + H2	1.0000E+18	-1.0000E+00	0.
		4.2458E+17	-7.3146E-01	-5.2130E+04
13	H + H + O2 = H2 + O2	1.0000E+18	-1.0000E+00	0.
		4.2458E+17	-7.3146E-01	-5.2130E+04
14	H + H + H2O = H2 + H2O	6.0000E+19	-1.2500E+00	0.
		2.5475E+19	-9.8146E-01	-5.2130E+04
15	H + OH + MPP = H2O + MPP	1.6000E+22	-2.0000E+00	0.
		7.2013E+22	-1.8355E+00	-5.9932E+04
16	H + O + MPP = OH + MPP	6.2000E+16	-6.0000E-01	0.
		1.4919E+16	-3.6131E-01	-5.1124E+04
17	OH + OH = O + H2O	5.7500E+12	0.	-3.9000E+02
		1.0490E+14	-7.1127E-02	-9.1938E+03

time increases. The code uses a static mesh with the breakpoints most closely spaced near the centre of integration interval and the flame front is forced to remain near the centre of integration interval. The error tolerance parameters SREC=1.0E-06 and E=1.0E-03 were used for runs reported in this study. SREC=1.0E-6 implies that the species having mass fraction of less than 1.0E-06 would be computed less accurately. E controls the tolerance for temporal errors and should be decreased as the number of breakpoints increase. For one run SREC-1.0E-08 and E=1.0E-06

5

were used. The results were not affected. The computational time increased by 4 times. The user can vary these parameters and obtain optimum values for his system which would give accurate solution as well as minimize the computing time.

3.3 FLAME SPEED

The flame speed as a function of H2 mole fraction (unburned mixture) for hydrogen-air flames have been reported by various workers. PLFLAME III calculates the flame speed from the species profile. Normally the time integration proceeds until the flame speed based on the changes in the major species profiles (reactants like H2, O2 and products like H2O) agree within a small fraction of a percent. Table 3 shows the comparison between the flame speed calculated by PLFLAME III code and those reported by Dixon-Lewis (3) and Warnatz(5). This table shows that the flame velocities calculated by the PLFLAME code are in fair agreement with those computed by Warnatz (5) and Dixon-Lewis (3) and the experimental data of Gunther and Janish (3). The qualitative trends are similar and maximum quantitative difference is around 50%.

TABLE 3

Mole Fraction Unburned Mix.	Flame	Speed Cm./Sec.		
H2/O2/N2	PLFLAME	Wartanaz (4)	Dixon-Lewis (3)	Gunther (3)
0.2/.17/.63	110.	100.	95.	152.
0.3/.15/.55	221.	245.	208.	280.
0.4/.126/.474	281	320.	258.	342.
0.5/.105/.395	253.	280.	239.	320.
0.6/.084/.316	179.	190.	152.	200.

The reasons for the differences between the experimental values and the computed values have been discussed in detail by Dixon-Lewis (3). The differences are attributed partly to the uncertainties in the values of rate constants and transport parameters but mostly to the experimental difficulties and errors such as existence of truly one dimensional flames, thermal disequilibrium, diffusion effects etc. Dixon-Lewis (3) considers

6

the experimental values of Gunther and Janish (3) to be too high. The
measured flame speed varies by a factor 0.65 to 1.4 from the mean flame
speed for Hydrogen-Air flames depending upon the experimental technique.(6)

3.4 COMPOSITION AND TEMPERATURE PROFILE

Dixon-Lewis (3) has reported measured composition profile and tempera-
ture profile for H_2-O_2-N_2 flame with unburned mole ratio of .188/.046/.766.
The surface temperature of the burner and the flow velocity has not been
reported by Dixon-Lewis (3). Therefore it was not possible to match the
absolute values of the axial distance between measured values and those
calculated by the PLFLAME code. The point for 15% change in H_2 profile
was matched between the calculated profiles (PLFLAME Code output) and the
experimental data of Dixon-Lewis and used as reference point for plotting.
The experimental data for H_2, O_2, H_2O and temperature profile from refer-
ence 3 are compared with the calculated results of PLFLAME code in Fig. 1
and Fig. 2. These figures show good agreement between the calculated
profiles and the experimental profiles in the primary flame zone (where
significant changes in composition and temperature take place). The flame
speed computed for this case by PLFLAME III is 9.7 cm./sec. as compared
to 9.2 cm/sec. reported by Dixon-Lewis (3).
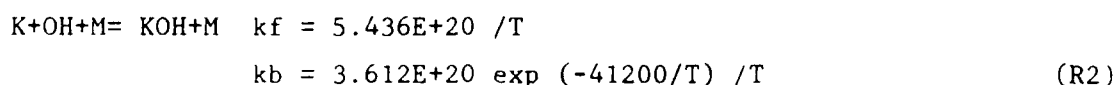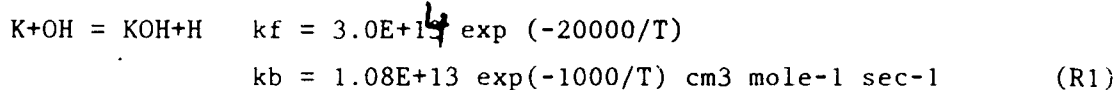
4.0 SENSITIVITY ANALYSIS

Coffee and Heimerl (7) have carried out a detailed sensitivity analysis
for PLFLAME Code varying the reaction rate coefficients and the transport
data. These changes produced expected trends in flame velocities and the
species mass fraction profiles. We were able to reproduce the results
of one of the four flames reported by Coffee and Heimerl (7) for the species
profile, temperature profile and the flame speed. The reaction rate for
the reaction $H+O_2 = OH+O$ was doubled in both directions and the PLFLAME
code was run. The computed flame speed increased from 253 to 306.7 cm/
sec. as per expectations. $H+O_2$ is a chain branching reaction producing
OH and O which react with H_2 and OH ultimately producing H_2O. The effect
of changes in the transport parameters produce the expected results as
discussed in reference 7.

From the above discussions and results it is reasonable to conclude
that PLFLAME Code calculations give good agreement with the results
reported by other workers and is caliberated for the available experimental

7

data for H2/02/N2 system. PLFLAME Code was used to study the effect of adding suppressant species K and KOH and on the computed flame velocity and the species profile.

4.1 EFFECT OF ADDING K TO H2/02/N2 FLAMES

PLFLAME Code was modified by adding the thermodynamic data and the kinetic rate data for the two inhibition reactions as suggested by the studies of Jensen and Jones (8-9):

K+OH = KOH+H   kf = 3.0E+14 exp (-20000/T)

   kb = 1.08E+13 exp(-1000/T) cm3 mole-1 sec-1   (R1)

K+OH+M= KOH+M   kf = 5.436E+20 /T

   kb = 3.612E+20 exp (-41200/T) /T   (R2)

PLFLAME code was run for the following compositions (unbounded flame).

TABLE 4

Run #	H2	02	N2	K
1.	.444	.111	.444	0.0
2.	.44	.11	.44	.01
3.	.433	.108	.433	.025
4.	.422	.106	.422	.050
5.	.413	.103	.413	.071

The mole ratio for H2/02/N2 is 4/1/4 for all these runs. The temperature profiles and composition profiles for H2, 02, H20, H and OH are shown in figs. 3 and 4 for 0% and 7.1%K. The flame speed variation is shown in table 5.

TABLE 5

%K	Flame Speed H2/02/N2 4/1/4 flame
0.0	259. cm./sec.
1.0	208.9
2.5	166.9
5.0	92.1
7.1	3.95

From table 5 we see that the flame speed decreases as the %K increases in the unburned mixture. The flame speed becomes negligible at 7.1% K which is in keeping with the expansion of the primary flame zone (as shown by the temperature profile and the composition profile in Figs. 3 and 4).

The inhibition effect of K is attributed to the stronger affinity of KOH for H atoms through the reaction $KOH+H = K+H2O$ as compared to that of O_2 through the chain branching reaction $H+O2 = OH+O$ resulting in decrease of H atoms in the primary flame zone. The peak mole fraction of H-atoms in the primary flame zone are as follows (Table 6):

TABLE 6

%K	H Atom Peak Mole Fract. H2/O2/N2 4/1/4 Flame
0.0	0.0626
1.0	0.0478
2.5	0.0313
5.0	0.0106
7.1	0.000756

Table 6 shows that the peak mole fraction of H Atom (as computed by the PLFLAME Code) decreases as the % of K in the unburnt mixture increases. The peak mole fraction of H atom decreases by an order of magnitude as %K increases from 5 to 7.1 and it is accompanied by a similiar decrease in flame velocity. Increasing the mole fraction of K beyond 7.1% does not have any discernible effect on the temperature profile and species profile. This would indicate that K reactions are very fast at 7.1% K flames and the controlling speed is shifted to the radical producing reaction of H2-O2 system.

4.2 EFFECT OF CHANGING THE REACTION RATE CONSTANTS FOR K,KOH,H Reactions:

The sensitivity of the inhibition effect to the values of the reaction rate constants involving K species is discussed in this section. The rate constants for the reactions R1 and R2 were changed by a factor of 10 (one at a time) and PLFLAME Code was run for various concentrations of K in the unburned gases.

4.2.1 Effect of Changing the Rate Constant for the Reaction KOH+H = K+H20

PLFLAME Code was run for the following conditions after increasing/ decreasing the rate constant for the reaction R1 by a factor of 10. The calculated flame speed results are shown in table 7:

Table 7

%K Addition	FLAME Baseline	SPEED CM/SEC Base Rate R1x10	Base Rate R1/10.
0.	259.0	259.0	259.0
2.5	166.9	162.7	185.0
5.0	92.1	83.8	144.0
7.1	7.0	3.25	109.6
10.	3.1	<1	22.6

The inhibition effect (in terms of decrease in flame speed and the expansion of the primary flame zone) of K is not stronlgy affected as the rate constant for the reaction KOH+H = K+H20 is increased by a factor of 10 (both foreward and backward). Thus it seems that the reaction R1 is sufficiently fast even with the baseline values and it is not the controlling step in determining the flame speed. The temperature profile and the composition profile do not show any change from the base line as the rate constant for the reaction R1 is increased by a factor of 10.

The inhibition effect of K decreases as the rate constant for the reaction R1 is decreased by a factor of 10 as is seen from the column 4 table 7. The temperature profiles and the composition profiles are steeper as compared to the corresponding profiles for the baseline value. Thus we see that the inhibition effect of K is not sensitive to the increase in the value of rate constant for the reaction R1. However the suppressant effect decreases some what as the rate constant for the reaction R1 decreases.

4.2.2 Sensitivity to the Rate Constant for Reaction K+OH+M=KOH+M

PLFLAME code was run after increasing/decreasing the rate constants for the reaction R2 by a factor of 10. The calculated flame speed results

are shown in table 8:

Table 8

%K Addition	FLAME SPEED CM/SEC		
	Baseline	Baseline R2x10	Baseline R2/10.
0.0	259.0	259.0	259.0
0.5	-	133.0	-
1.0	208.9	-	-
2.5	166.9	8.1	-
5.0	92.1	-	207.5
7.1	3.95	-	188.
10.0	3.1	-	3.49

This table 8 shows that the inhibition effect of K increases as the rate constant for the reaction R2 is increased by a factor of 10. The inhibition effect at 2.5% K addition to the unburned gases is similar to that of 7% K addition at the baseline value of rate constant for the reaction R2. When the rate constant for the reaction R2 is decreased by a factor of 10 the inhibition effect of K decreases significantly up to 7.1% K addition. At 10% K addition the inhibition effect of K (with rate R2 = baseline rate/10) is similar to that of 7.1% K addition with the baseline values. Thus it appears that for Hydrogen rich air flames the inhibition effect of K is more sensitive to the rate constant for reaction R2. This needs to be verified experimentally. The above results also show that the addition of KOH would have a stronger inhibition effect as compared to that of K with the same % addition. This is confirmed by the following results.

4.2.3 Effect of KOH Addition

PLFLAME Code was run for 1% KOH and 2.5% KOH addition to the unburnt gases. The flame speed variation are as follows:

Table 9
FLAME SPEED H2/02/N2 4/1/4

% Addition	K	KOH
0.0	259	259 cm/sec
1.0	208	194
2.5	166.7	8.1
7.1	3.3	-

From this we see that the inhibition effect of 2.5% KOH is similar to that of 7.1% K addition to the unburnt gases. This is confirmed by the temperature and composition profiles. These results need to be confirmed from the experimental measurements in the flame apparatus near completion at the AFRPL.

4.3 BURNER STABLISED FLAMES

PLFLAME Code was run for the burner stablised flames by giving appropriate values to the input parameters such as gas flow speed, burner surface temperature. The program was run for 3 different values of the burner surface temperatures and 3 different values of gas flow velocity. In the limiting case when the flow velocity was greater than the flames speed, the flame did not ignite as expected and gave additional confidence to the realiability of the program. The composition profiles and the temperature profiles need to verified against the experimental measurements.

5.0 SUMMARY AND CONCLUSIONS

* PLFLAME Code gives satisfactory results.

* The calculated flame speeds, temperature profile and the composition profile in good agreement those measured experimentallty for H2/02/N2 system.

* The flame speed decreases as the % of K in the unburned H2/02/N2 mixture increases.

* The length of the primary increases as in the % of K increases.

* There is no change in the inhibition effect as the % of K is increased from 7% to 10% in the unburned H2/02/N2 mixture.

* The inhibition effectof 2.5% KOH addition is similar to that of 7% K addition to the H2/02/N2 4/1/4 mixture.

* The inhibition effect of K is more sensitive to the rate constant

of the reaction K+OH+M = KOH+M as compared to that of reaction KOH+H = K+H2O.

* These results for H2/O2/N2/K systems need to be verified experimentally.

REFERENCES

1   Herimerl, J.M. and Coffee, T.P., "The Detailed Modeling of Premixed Laminar
     Steady-State Flames," Combustion and Flame 39: 301-315C1980.

2.   Coffee, T.P., "A Computer Code for the Solution of the Equations Governing
     a Laminar, Premixed One-Dimensional Flame, "Report ARBRL-MR-03265, US Army
     Ballistic Research Laboratory, Aberdeen Proving Ground, MD 21005, April,
     1982.

3.   Dixon-Lewis, G. "Kinetic Mechanism, Structure and Properties of Premixed
     Flames in Hyrdrogen-Oxygen-Nitrogen Mixtures", Proceedings, Royal Society
     London, Vol. 292, pp. 45-99, 1979.

4.   Jensen, D.E. and Jones, G.A., "Kinetics of Flames Inhibition by Sodium,"
     J. Chem. Soc. Faraday Trans. 1, 1982, 78.

5.   Warnatz, J. "Calculation of the Structure of Laminar Flat Flames II; Flame
     Velocity and Structure of Freely Propagating Hydrogen-Oxygen and Hydrogen-
     Air Flames," Phys. Chem. 82, 643-649 (1978).

6.   Andrews G.E., Brandy D. "Determination of Burning Velocities: A Critical
     Review," Combustion and Flame 18, pp. 133-153 (1972).

7.   Coffee, T.P. and Heimerl, J.M. "Sensitivity, Analysis For Premixed Laminar,
     Steady State Flames," Report ARBRL-TR-02437, US Army Ballistie Research
     Laboratory, Aberdeen Proving Ground, MD, January, 1983.

8.   Jensen, D.E. and Jones, G.A. "Kinetics of Flame Inhibition by Potassium",
     J. Chem. Soc. Faraday Trans. 1, 1982, 78.

9.   Jensen, D.E, "Alkali Compounds in Oxygen-rid Flames", J. Chem. Soc.
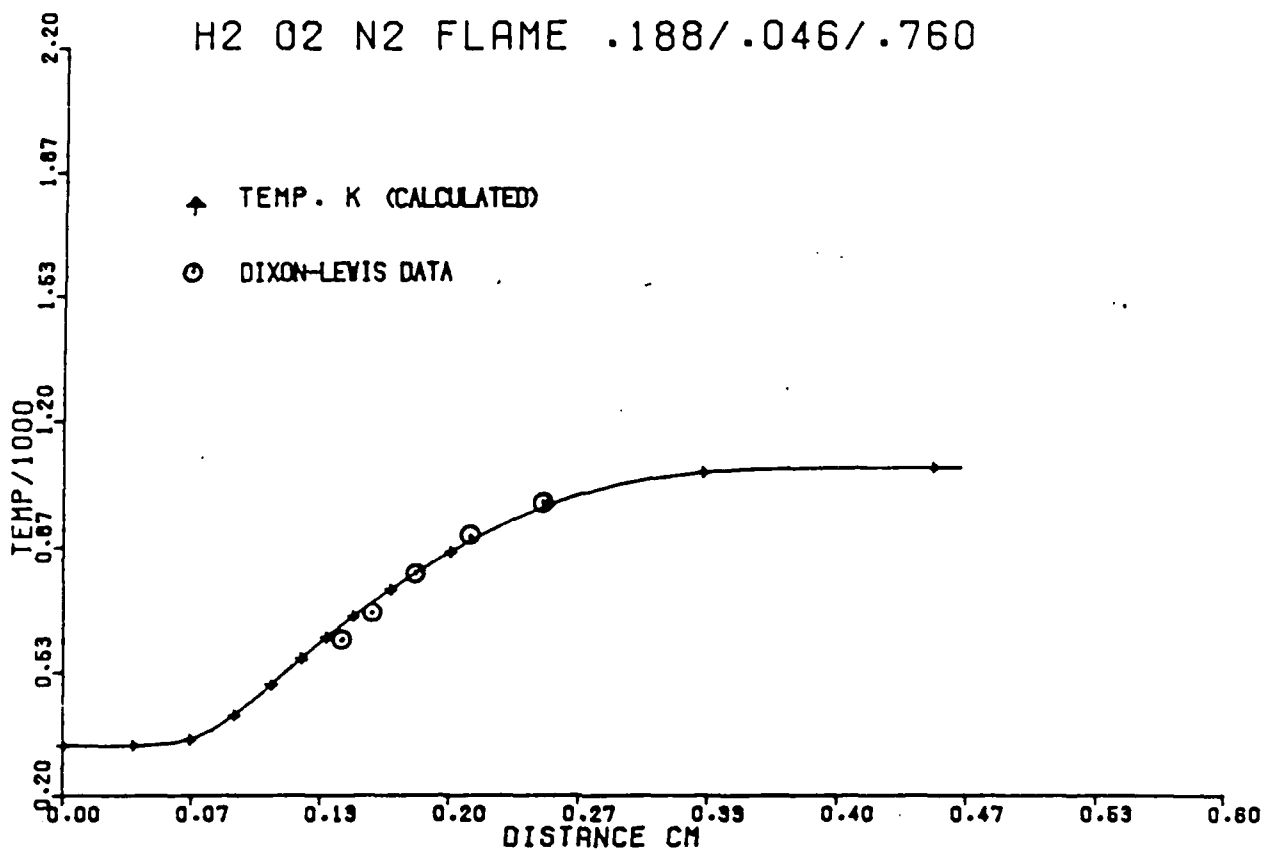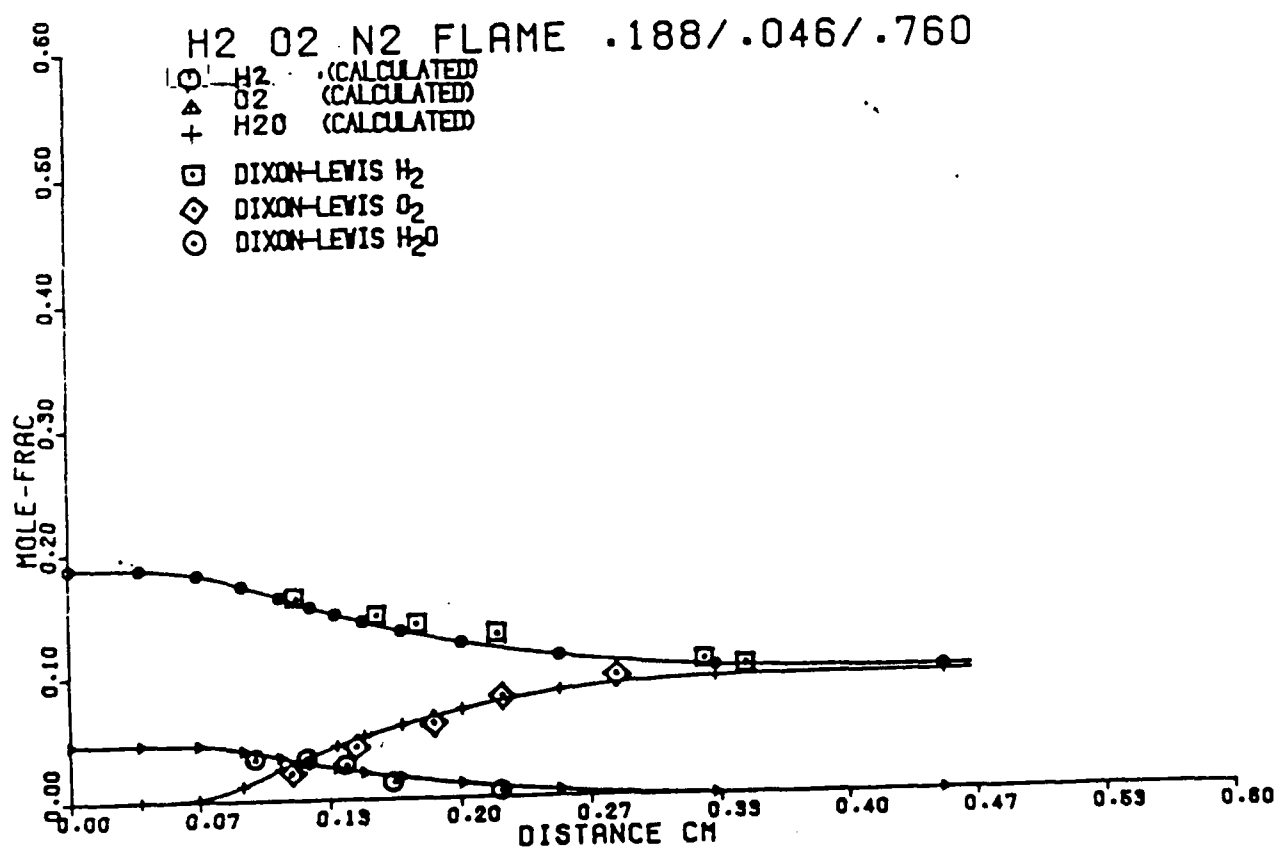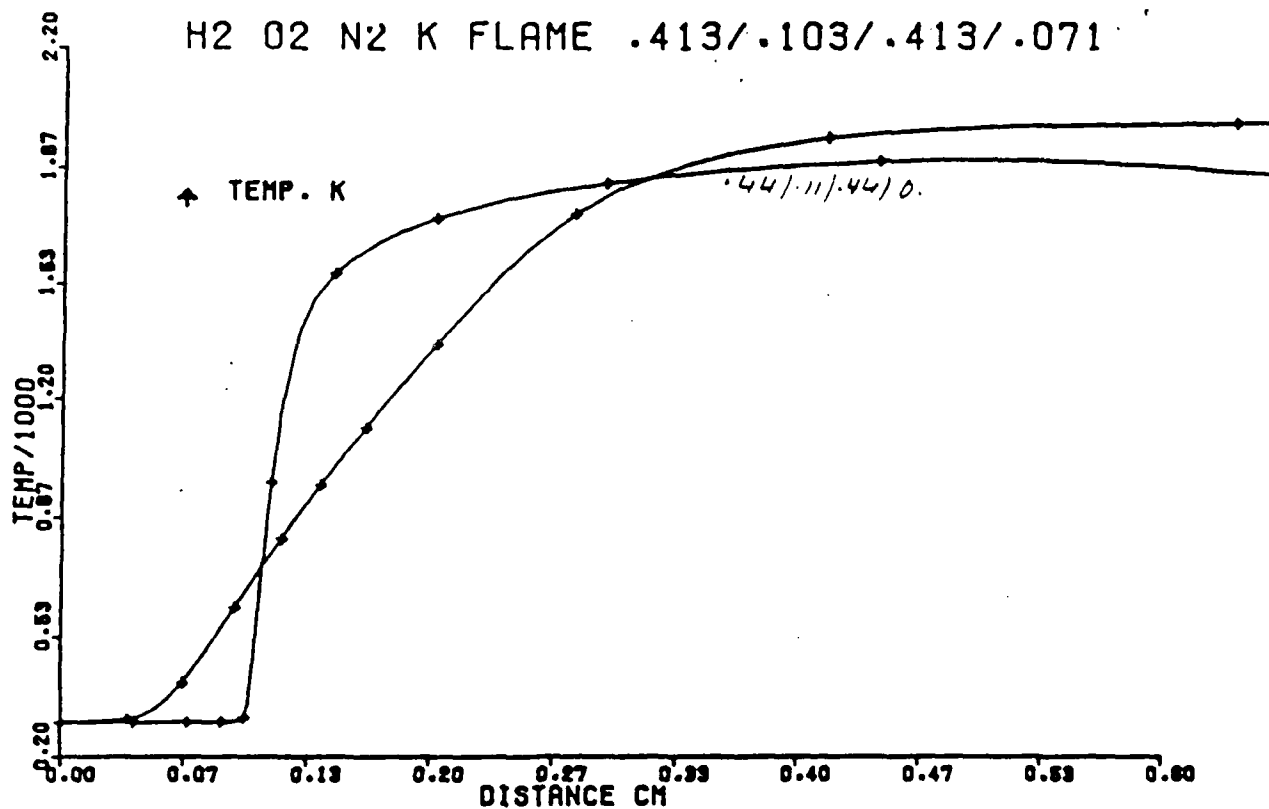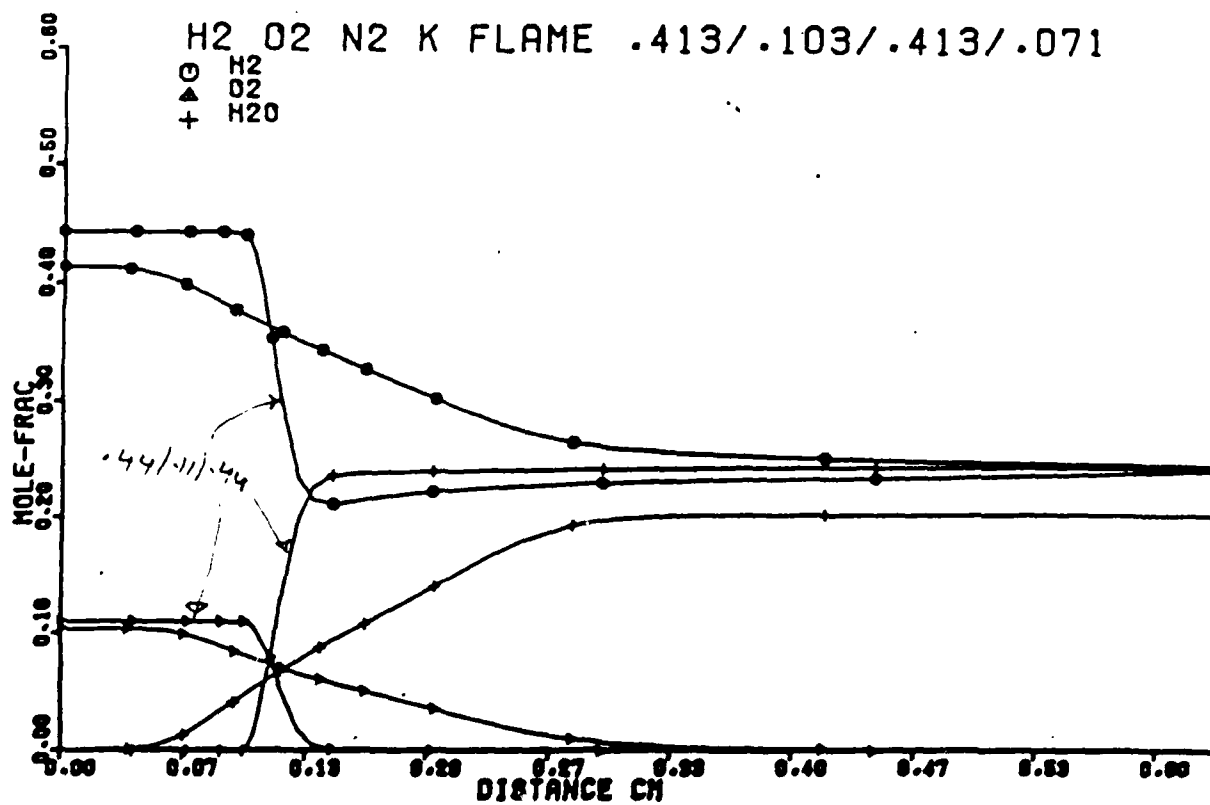   Fraday Trans. 1, 1982, 78.

H2 02 N2 FLAME .188/.046/.760

Fig 1

H2 02 N2 FLAME .188/.046/.760

Fig 2

H2 O2 N2 K FLAME .413/.103/.413/.071

Fig 3

H2 O2 N2 K FLAME .413/.103/.413/.071

Fig 4